Differential Requirements for Core2 Glucosaminyltransferase for Endothelial L-Selectin Ligand Function In Vivo[1]

Markus Sperandio,* S. Bradley Forlow,* Jayant Thatte,* Lesley G. Ellies,‡ Jamey D. Marth,‡ and Klaus Ley[2]*†

L-selectin is a calcium-dependent lectin on leukocytes mediating leukocyte rolling in high endothelial venules and inflamed microvessels. Many selectin ligands require modification of glycoproteins by leukocyte core2 β1,6-*N*-acetylglucosaminyltransferase (Core2GlcNAcT-I). To test the role of Core2GlcNAcT-I for L-selectin ligand biosynthesis, we investigated leukocyte rolling in venules of untreated and TNF-α-treated cremaster muscles and in Peyer's patch high endothelial venules (HEV) of Core2GlcNAcT-I null (core2$^{-/-}$) mice. In the presence of blocking mAbs against P- and E-selectin, L-selectin-mediated leukocyte rolling was almost completely abolished in cremaster muscle venules of core2$^{-/-}$ mice, but not littermate control mice. By contrast, leukocyte rolling in Peyer's patch HEV was not significantly different between core2$^{-/-}$ and control mice. To probe L-selectin ligands more directly, we injected L-selectin-coated beads. These beads showed no rolling in cremaster muscle venules of core2$^{-/-}$ mice, but significant rolling in controls. In Peyer's patch HEV, beads coated with a low concentration of L-selectin showed reduced rolling in core2$^{-/-}$ mice. Beads coated with a 10-fold higher concentration of L-selectin rolled equivalently in core2$^{-/-}$ and control mice. Our data show that endothelial L-selectin ligands relevant for rolling in inflamed microvessels of the cremaster muscle are completely Core2GlcNAcT-I dependent. In contrast, L-selectin ligands in Peyer's patch HEV are only marginally affected by the absence of Core2GlcNAcT-I, but are sufficiently functional to support L-selectin-dependent leukocyte rolling in Core2GlcNAcT-I-deficient mice. ***The Journal of Immunology*****, 2001, 167: 2268–2274.**

Leukocytes are migratory cells characterized by their ability to leave the vascular system and transmigrate into sites of inflammation or into lymphoid tissue during lymphocyte homing. The recruitment of leukocytes requires a multistep adhesion cascade that begins with leukocyte capture and rolling and leads to firm adhesion and transmigration (1–3). The early steps of leukocyte recruitment, capture, and rolling are largely mediated by E-, P-, and L-selectin (4). L-selectin (CD62L) is constitutively expressed on most leukocytes, including granulocytes, monocytes, and naive and some memory lymphocytes.

Observation of inflamed venules in vivo has shown that leukocytes (5, 6) and L-selectin transfectants (7) can roll by binding to unidentified endothelial L-selectin ligands. Usually, L-selectin cooperates with P- and E-selectin to mediate rolling, but L-selectin-dependent rolling can be isolated in E/P$^{-/-}$ mice (8) or in mice in which P- and E-selectin are blocked by mAbs (9). The physiologically relevant L-selectin ligands in inflamed venules are unknown. L-selectin ligand activity can be induced by cytokine treatment of cultured endothelial cells (10), but the relevant glycoprotein bearing the ligand has not been identified. L-selectin ligands on inflamed endothelial cells express fucosylation-dependent epitopes such as HECA452 (11). In addition, sensitivity to chlorate treatment (12) and data from two newly identified carbohydrate sulfotransferases, CHST1 and CHST2 (13), suggest that sulfotransferase activity is required for L-selectin ligand expressed by inflamed venules.

In high endothelial venules (HEV)[3] of secondary lymphoid organs, L-selectin is the predominant selectin mediating leukocyte rolling (14). The importance of L-selectin for lymphocyte trafficking is evident in L-selectin-deficient mice. These mice show small, lymphocyte-depleted peripheral lymph nodes with reduced binding of lymphocytes to HEV using the Stamper-Woodruff assay (15). L-selectin is also required for most leukocyte rolling in Peyer's patch HEV (16), but $\alpha_4\beta_7$ integrin mediates sufficient rolling in L-selectin-deficient mice to ensure normal size and cellularity of Peyer's patches.

L-selectin ligands on HEV of secondary lymphoid organs require carbohydrate-based post-translational modifications for recognition. Similar to ligands for P- and E-selectin, L-selectin ligands are thought to carry sialylated and fucosylated sequences on core2 β1,6-*N*-acetylglucosaminyltransferase (Core2GlcNAcT-I)-modified *O*-linked glycans (17, 18). L-selectin ligands on HEV also require sulfation on C-6 of *N*-acetylglucosamine and/or C-6 of galactose of sialyl Lewis x (sLe^x) (19, 20). The L-selectin ligand function of HEV can be blocked by the carbohydrate-binding mAb MECA-79, which helped to identify candidate L-selectin ligands on HEV, including glycosylation-dependent cell adhesion molecule-1 and CD34 (21). It is thought that L-selectin ligands on HEV are distinct from those expressed on inflamed venules.

Because of the transient nature of the bond formed between L-selectin and its ligands, the direct demonstration of functional

*Department of Biomedical Engineering, and †Cardiovascular Research Center, University of Virginia, Charlottesville, VA 22908; and ‡Howard Hughes Medical Institute, University of California, La Jolla, CA 92119

Received for publication March 13, 2001. Accepted for publication June 6, 2001.

The costs of publication of this article were defrayed in part by the payment of page charges. This article must therefore be hereby marked *advertisement* in accordance with 18 U.S.C. Section 1734 solely to indicate this fact.

[1] This work was supported by National Institutes of Health Grants HL64381 and HL54136 (to K.L.) and National Institutes of Health Grant DK48247 (to J.D.M.). M.S. is supported by a stipend from the German Research Foundation (SP 621/1-1). L.G.E. is supported by National Cancer Institute Award K08-CA88035.

[2] Address correspondence and reprint requests to Dr. Klaus Ley, Department of Biomedical Engineering, University of Virginia Health Sciences Center, Box 377, Charlottesville, VA 22908. E-mail address: kfl3@virginia.edu

[3] Abbreviations used in this paper: HEV, high endothelial venule; FucT, fucosyltransferase; Core2GlcNAcT-I, core2 β1,6-*N*-acetylglucosaminyltransferase; core2$^{-/-}$, Core2GlcNAcT-I deficient.

0022-1767/01/$02.00

L-selectin ligands has been difficult (22). To circumvent this problem, gene-targeted mice have been developed lacking glycosylation enzymes such as fucosyltransferase VII (FucT-VII) (23) and IV (24) or Core2GlcNAcT-I (25). Fucosyl and Core2GlcNAc transferases are likely to be involved in the post-translational modification of functional L-selectin ligands. Gene targeting shows that FucT-VII, but not FucT-IV, is required for L-selectin ligand activity in HEV (23, 24). Recent work by Ellies et al. (25) using a parallel plate flow chamber-controlled detachment assay provided evidence that leukocytes isolated from Core2GlcNAcT-I-deficient mice (core2$^{-/-}$) show reduced rolling on L-selectin. This finding addresses leukocyte L-selectin ligands, but not endothelial L-selectin ligands.

The present study was designed to investigate endothelial L-selectin ligand function in the absence of leukocyte Core2GlcNAcT-I. To this end we investigated L-selectin-dependent leukocyte rolling in unstimulated and TNF-α-stimulated cremaster muscle venules. In cremaster muscle venules mild trauma caused by exteriorization of the cremaster muscle leads to induction of leukocyte rolling that is initially P- and later also L-selectin dependent (26). TNF-α treatment leads to L-selectin-mediated rolling starting at >4 h after TNF-α administration (8). In addition, L-selectin-mediated rolling was studied in high endothelial venules of Peyer's patches.

Materials and Methods

Animals

Mice lacking a functional gene encoding the leukocyte Core2GlcNAcT-I (EC 2.4.1.102) were generated as described previously (25) and maintained as a heterozygous breeding colony at the University of Virginia (Charlottesville, VA). The wild-type Core2GlcNAcT-I allele was detected using PCR primers located adjacent to the deleted region (W5′, 5′-GGGTTACGGAT GAGCTCTGTGTC; W3′, 5′-CCCTGGAAGCAAGGACAATTCTG-3′), resulting in a 304-bp fragment, while the mutant allele was detected using W5′ and a *lox*P primer (M3′, 5′-CTCGAATTGATCCCCGGGTAC-3′), yielding a 200-bp fragment. Control experiments were performed in heterozygous (+/−) and homozygous (+/+) littermates. All experiments were performed on healthy mice that were at least 8 wk of age. All mice were housed in a barrier facility under specific pathogen-free conditions. All animal experiments were approved by the institutional animal care and use committee.

Abs and cytokines

The P-selectin mAb RB40.34 (rat IgG1, 30 μg/mouse) blocking P-selectin-dependent adhesion and recruitment (27) and P-selectin-dependent leukocyte rolling in vivo (26) was a gift from Dr. D. Vestweber (University of Munster, Munster, Germany). mAb 9A9 was a gift from Dr. B. Wolitzky (Hoffman-LaRoche, Nutley, NJ) and blocks E-selectin-mediated rolling in vivo (9). The L-selectin mAb MEL-14 (rat IgG2a, 50 μg/mouse) was purified from hybridoma supernatant (American Type Culture Collection, Manassas, VA). This Ab blocks L-selectin-dependent leukocyte rolling in vivo (16, 26). The mAb PS/2 is specific for the α_4 integrin chain (rat IgG 2b; 30 μg/mouse) and was purified from hybridoma supernatant (American Type Culture Collection). This mAb blocks $\alpha_4\beta_7$-dependent binding of lymphocytes to recombinant mucosal addressin cell adhesion molecule-1 in vitro (28) and lymphocyte homing to Peyer's patches in vivo (29).

L-selectin IgG chimera coupled microbeads in vivo

A murine L-selectin IgG fusion protein (30) (provided by Dr. Susan Watson) was bound to protein G-coupled fluorescent 2-μm microbeads (Polysciences, Warrington, PA) and injected into mice as described previously (16). Briefly, recombinant protein G (Sigma, St. Louis, MO) was covalently coupled to fluorescent-carboxylated (2-μm diameter) YG microspheres using a carbodiimide-coupling kit according to the manufacturer's directions (all from Polysciences). One hour before use, 25 μl protein G-coupled beads were washed in PBS and mixed with either PBS-1% BSA solution (control beads) or two different concentrations of the L-selectin IgG chimera (10 μg/ml for L^{low} and 100 μg/ml for L^{high}). The mixture was allowed to incubate for 1 h, washed in PBS-1% BSA, resuspended in 0.3 ml isotonic saline, and vortexed. Injection of control, L^{low}, and L^{high} beads was performed after pretreatment with the P-selectin-blocking mAb RB40.34. Almost all circulating beads were cleared within 5–10 min following injection. As a specificity control, L^{high} beads were injected after pretreatment with L-selectin-blocking mAb MEL-14 (50 μg/ml).

Flow cytometry

Flow cytometry was used to detect L-selectin expression on peripheral blood leukocytes of control and Core2GlcNAcT-I-deficient mice and on microbeads coated with L-selectin chimera. The preparation of L-selectin-coupled beads was performed with carboxylated (2 μm diameter) nonfluorescent YG microspheres as described above. Whole blood was centrifuged, and RBC lysis was conducted with PharM-Lyse-10X solution (PharMingen, San Diego, CA). Blood cells were suspended in PBS-1% BSA (Sigma) solution and incubated in the dark with either MEL-14 conjugated with PE or rat IgG2a conjugated with PE (both from PharMingen) for 30 min on ice (0.5 μg/10^6 cells). Subsequently, cells were washed twice in PBS-1% BSA solution and then incubated with FITC-conjugated mAb Ly-6G directed against the neutrophilic surface Ag GR-1 (PharMingen) for 30 min on ice (0.5 μg/10^6 cells). L-selectin-coated microbeads and control microbeads were suspended in PBS-1% BSA solution and incubated with goat serum (2 μl/10^6 cells) for 30 min on ice to block unspecific binding sites. Thereafter, beads were washed twice in PBS-1% BSA solution and incubated with either MEL-14 conjugated with PE or rat IgG2a conjugated with PE (both from PharMingen) for 30 min on ice (0.5 μg/10^6 cells). L-selectin expression on cells and beads was determined on 10,000 leukocytes/beads per mouse using a 4-decade FACScan with the CellQuest software package (Becton Dickinson, San Jose, CA).

Intravital microscopy

Mice were anesthetized with i.p. injection of ketamine (125 mg/kg body weight; Ketalar; Parke-Davis, Morris Plains, NJ), xylazine (12.5 mg/kg body weight; Phoenix Scientific, St. Joseph, MO), and atropin sulfate (0.25 mg/kg body weight; Elkins-Sinn, Cherry Hill, NJ) and placed on a heating pad to maintain body temperature.

Microscopic observations were conducted on an intravital microscope (Axioskop; Zeiss, Thornwood, NY) with a saline immersion objective (SW 40/0.75 numerical aperture). The trachea was intubated, followed by cannulation of the right jugular vein for administration of anesthetic. Thereafter, the left carotid artery was cannulated for blood pressure monitoring, blood samples, and systemic mAb injections. Blood pressure was monitored intermittently during the experiment (model BPMT-2; Stemtech, Menomonee Falls, WI). During the experiment mice received 0.2 ml/h, diluted pentobarbital in saline i.v. to maintain anesthesia, and a neutral fluid balance.

Cremaster muscle preparation

The cremaster muscle was prepared for intravital microscopy as previously described (9). Microscopic observation was conducted on postcapillary venules ranging from 20–50 μm in diameter. The epididymis and testis were gently pinned to the side, and the cremaster muscle was superfused with thermocontrolled (35°C) bicarbonate-buffered saline. To detect possible changes in systemic white blood cell count after injection of the various Abs, systemic blood samples (10 μl) were taken after each mAb injection. Blood samples were diluted 1:10 with Kimura (11 ml 5% (w/w) toluidine blue, 0.8 ml 0.03% light green SF yellowish, 0.5 ml saturated saponin, and 5 ml 0.07 M phosphate buffer, pH 6.4; all from Sigma) and analyzed for leukocyte concentration (expressed as number of leukocytes per microliter of whole blood).

Peyer's patch preparation

A Peyer's patch was prepared for intravital microscopy as described previously (31, 32). Briefly, a 1.5-cm incision was made along the linea alba to open the peritoneal cavity and expose the cecum and small intestine. The mouse was then turned on its side, and the intestines were pushed out of the peritoneal cavity by gently pressing on the back. The intestines were superfused with thermocontrolled (35°C) bicarbonate-buffered saline as previously described. The small intestine was placed between two parallel strips of clear silicone, high vacuum grease (Dow Corning, Midland, MI) on a plastic coverslip (Baxter, Deerfield, IL). To visualize intravascular leukocytes by epifluorescence microscopy, each mouse was given a 0.15-ml i.v. injection of 2 mg/ml rhodamine 6G (Molecular Probes, Eugene, OR) 15 min before intravital microscopy. The intravital microscope (Axioskop; Zeiss) was equipped with a saline immersion objective (SW 63/0.9 numerical aperture). For observation of Peyer's patch HEV, epifluorescence illumination (60/s; Strobex 236; Chadwick Helmuth, Mountain View, CA), and filter block Zeiss 9) was used. Each venule was observed for 60 s. Venules with diameters between 12 and 35 μm were observed and

recorded via a CCD camera system (model VE-1000CD, Dage-MTI, Michigan City, IN) on a Panasonic S-VHS recorder (Panasonic, Secaucus, NJ).

Data analysis

Microvessel diameter and length were measured using a digital image processing system (33). Centerline RBC velocity in the cremaster muscle preparation was measured using a dual photodiode and a digital on-line cross-correlation program (Circusoft Instrumentation, Hockessin, DE). Centerline velocities were converted to mean blood flow velocities by multiplying with an empirical factor of 0.625 (34). Centerline blood flow velocity in venules of Peyer's patches was determined after i.v. injection of 2-μm diameter fluorescent YG microspheres (Polysciences) by measuring frame-to-frame displacement of single beads (three microspheres per venule). Wall shear rates (γ_w) were estimated as 2.12 ($8v_b/d$), where v_b *is the mean blood flow velocity,* d is the diameter of the vessel, and 2.12 is a median empirical correction factor obtained from actual velocity profiles measured in microvessels in vivo (35).

The rolling leukocyte flux fraction was determined as the number of rolling leukocytes expressed as a percentage of all leukocytes passing through the venule per unit time. Rolling flux fraction in cremaster muscle venules was calculated as previously described (26) by dividing leukocyte rolling flux by total leukocyte flux estimated as [WBC] $v_b\ \pi\ (d/2)^2$, where [WBC] is the actual systemic leukocyte count, v_b is the blood flow velocity, and d is the venular diameter. In Peyer's patch HEV, the number of rolling leukocytes was consistently higher (by 60%) than the product of the flow rate and the systemic leukocyte concentration, possibly because of the preferential delivery of leukocytes to the terminal capillaries in microvascular networks (36, 37). The flux fraction in venules of Peyer's patch from untreated control mice was set at 100%, and the flux fractions in mAb-treated controls and in untreated and mAb-treated Core2GlcNAcT-I-deficient mice were expressed relative to control.

Statistics

Statistical analysis was performed using SigmaStat 2.0 software package (SPSS, Chicago, IL). Average vessel diameter, leukocyte rolling flux fractions, leukocyte rolling velocities, and shear rates between groups and treatments were compared by one-way ANOVA on ranks (Kruskal-Wallis) with a multiple pairwise comparison test (Dunn's test). Leukocyte counts and differentials were compared with Student's t test or by the Wilcoxon rank-sum test as appropriate. Statistical significance was set at $p < 0.05$, indicated by an asterisk.

Results

Core2$^{-/-}$ mice were fertile and healthy under vivarium conditions. There was no difference in systemic blood pressure between core2$^{-/-}$ mice and control mice (Table I). Systemic leukocyte counts were significantly higher in core2$^{-/-}$ mice than in control mice ($p < 0.05$; Table I). This was mainly due to a significantly higher number of polymorphonuclear cells in core2$^{-/-}$ mice ($p < 0.05$; Table I) and is consistent with similar results reported previously (25, 38).

Leukocyte rolling in untreated venules of the cremaster muscle

We analyzed leukocyte rolling in 41 venules of six core2$^{-/-}$ mice and compared the results to those in 13 venules of three littermate controls. Microvascular parameters between Core2GlcNAcT-I-deficient mice and control mice are presented in Table II and show no significant differences regarding diameter, blood flow velocity, and wall shear rate. Leukocyte rolling in untreated venules is initially P-selectin dependent (26, 39), followed by a second phase that begins 1 h after exteriorization that is both L-selectin and P-selectin dependent (26, 40). To study L-selectin-dependent rolling, the P-selectin-blocking mAb RB40.34 was injected into control mice at >60 min after exteriorization. This completely eliminated rolling during the first hour (data not shown) and led to a marked decrease in rolling flux fraction from 23 to 4% at later times (Fig. 1). The residual rolling was completely L-selectin dependent, as confirmed by blocking residual rolling after injection of L-selectin blocking Ab MEL-14 (Fig. 1).

Table I. *Systemic arterial blood pressure, systemic leukocyte counts, and PMN differential in untreated and TNFα-treated mice*[a]

	Mice (n)	Systolic Blood Pressure (mm Hg)	Systemic Leukocyte Count (cells/μl)	PMN (%)
Core2$^{-/-}$	28	86 ± 3	5800 ± 400	47 ± 4
Control	18	89 ± 4	3500 ± 300	34 ± 5
		NS	$p < 0.05$	$p < 0.05$

[a] Systemic arterial blood pressure, systemic leukocyte count, and PMN are presented as mean ± SEM.

In untreated Core2GlcNAcT-I-deficient mice, we observed a dramatically reduced rolling flux fraction of 3%, which was totally blocked by the injection of P-selectin-blocking mAb RB40.34 >60 min after exteriorization (Fig. 1). The absence of leukocyte rolling in P-selectin-blocking mAb RB40.34-treated core2$^{-/-}$ mice shows that L-selectin-mediated rolling in this model is completely Core2GlcNAcT-I dependent.

Leukocytes of gene-targeted mice with null mutations for certain adhesion molecules (41, 42) exhibit a lower surface expression of L-selectin. To exclude the possibility that a different L-selectin expression on leukocytes accounts for the absence of L-selectin-mediated rolling in core2$^{-/-}$ mice, L-selectin expression was analyzed in peripheral blood leukocytes by flow cytometry. We found that L-selectin expression was similar in Core2GlcNAcT-I-deficient and control mice (Fig. 2, *A* and *B*).

To directly show that L-selectin ligand expression in cremaster muscle venules is severely affected by the absence of Core2GlcNAcT-I, microbeads coated with L-selectin at a low (10 μg/ml, L^{low}) or a high (100 μg/ml, L^{high}) concentration of L-selectin IgG-chimera were injected into the left carotid artery. Coupling of the L-selectin chimera to the beads was verified by flow cytometry (Fig. 2, *C* and *D*). The L-selectin concentration on L^{low} beads (Fig. 2*C*) was similar to the L-selectin expression observed on leukocytes of core2$^{-/-}$ mice or control mice. L^{high} beads had a stronger intensity signal (Fig. 2*D*) than leukocytes. Rolling of microbeads in vivo was analyzed in 26 venules of nine core2$^{-/-}$ mice and compared with rolling in 23 venules of eight control mice. Injected control beads showed no detectable rolling in venules of the cremaster muscle in either core2$^{-/-}$ or control mice (Fig. 3). Injection of L^{low} microbeads into control mice showed some rolling in cremaster muscle venules (3%), which increased to 6% for L^{high} microbeads (Fig. 3). In contrast, no rolling was observed after injection of either L^{low} or L^{high} microbeads into cremaster muscle venules of core2$^{-/-}$ mice (Fig. 3). This confirms that L-selectin ligands are not functional in inflamed venules of core2$^{-/-}$ mice.

Long term (>4 h) TNF-α-induced inflammation

Treatment with TNF-α for 4 h or more leads to significant L-selectin-mediated rolling that is sufficient for near-normal leukocyte recruitment (8). We assessed leukocyte rolling in 46 venules of 10 TNF-α-treated (4–6 h) mice lacking Core2GlcNAcT-I and compared the results to rolling in 16 venules of four control animals. Microvascular parameters for both groups are presented in Table II and show similar results for vessel diameter, centerline velocity, and wall shear rate. Leukocyte rolling flux fraction after TNF-α treatment was reduced to 10% in untreated core2$^{-/-}$ mice from 27% in untreated control mice ($p < 0.05$; Fig. 4*A*). Injection of both the P-selectin-blocking mAb RB40.34 and the E-selectin-blocking mAb 9A9 into core2$^{-/-}$ mice removed almost all rolling cells, whereas significant rolling remained in the control group (rolling flux fraction, 7%; $p < 0.05$; Fig. 4*A*). The residual rolling

Table II. *Microvascular parameters in cremaster muscle venules of untreated and TNFα-treated mice and in HEV of Peyer's patches*[a]

Mouse Genotype	Mice (*n*)	Venules (*n*)	Diameter (μm)	Centerline Velocity (mm/s)	Wall Shear Rate (s^{-1})
Untreated cremaster					
Core2$^{-/-}$	6	41	37 ± 2	3.6 ± 0.4	1100 ± 100
Control	3	13	32 ± 2	3.7 ± 0.4	1300 ± 200
			NS	NS	NS
TNF-α-treated cremaster					
Core2$^{-/-}$	10	46	36 ± 1	2.3 ± 0.2	680 ± 60
Control	4	16	34 ± 2	1.9 ± 0.2	580 ± 70
			NS	NS	NS
Untreated Peyer's patch					
Core2$^{-/-}$	12	31	19 ± 1	1.6 ± 0.2	880 ± 80
Control	11	35	19 ± 1	1.3 ± 0.1	740 ± 60
			NS	NS	NS

[a] Diameters, centerline velocity, and wall shear rate are presented as mean ± SEM.

in control mice was completely blocked by injection of the L-selectin-blocking mAb MEL-14 (Fig. 4*A*). This provides direct evidence that TNF-α-induced L-selectin ligands are completely Core2GlcNAcT-I dependent.

To further characterize L-selectin-dependent rolling in this model, we investigated leukocyte rolling velocity distributions in TNF-α-treated cremaster muscle venules. TNF-α-treated core2$^{-/-}$ mice showed an average rolling velocity of 11 ± 1 μm/s, identical with that of control mice (11 ± 1 μm/s; Fig. 4*B*). Injection of P-selectin-blocking mAbRB40.34 and E-selectin-blocking mAb 9A9 led to a significant increase in rolling velocity in control mice (59 ± 8 μm/s; Fig. 4B). This suggests a higher rolling velocity for L-selectin-mediated rolling in this model, similar to findings in cremaster muscle venules not treated with TNF-α (8). Core2GlcNAcT-I-deficient mice injected with blocking mAbs against P- and E-selectin showed no rolling.

Leukocyte rolling in high endothelial venules of Peyer's patch

Leukocyte rolling was analyzed in 39 venules of 11 core2$^{-/-}$ mice and compared with rolling in 35 venules in 12 control mice. Microvascular parameters are presented in Table II and show no significant differences regarding vessel diameter, centerline velocity, and wall shear rate. In control mice, injection of the P-selectin mAb RB40.34 led to a modest decrease in the rolling flux fraction from 100 to 84% (Fig. 5), which confirms earlier observations of a contribution of P-selectin to rolling in this setting (16). In untreated core2$^{-/-}$ mice, the rolling flux fraction also was slightly reduced by injection of P-selectin-blocking mAb RB40.34 into core2$^{-/-}$ mice (from 84 to 74%). Injection of the L-selectin-blocking mAb MEL-14 into core2$^{-/-}$ mice reduced leukocyte rolling to 14%, similar to the rolling flux fraction seen in MEL-14-treated control mice (18%; Fig. 5). This demonstrates that Core2GlcNAcT-I deficiency does not detectably impair L-selectin-mediated rolling in Peyer's patch HEV. Injection of P-selectin-blocking mAb RB40.34 and L-selectin-blocking mAb MEL-14 reduced rolling flux fraction to 10% in controls and 9% in core2$^{-/-}$ mice, respectively (Fig. 5). The residual rolling was entirely α_4 integrin dependent, because it was completely abolished by the additional injection of the α_4 integrin-blocking mAb PS/2 (Fig. 5).

For a more detailed investigation of L-selectin ligands in Peyer's patch HEV, we injected L-selectin-coated microbeads and assessed rolling of the beads in high endothelial venules. L^{low} microbeads rolled (rolling flux fraction, 13%) in core2$^{-/-}$ mice. However, this rolling was reduced from a rolling flux fraction of 50% in control mice (Fig. 6). The lower rolling flux fraction of L^{low} microbeads in core2$^{-/-}$ mice suggests a somewhat decreased activity of L-selectin ligands on Peyer's patch HEV of core2$^{-/-}$ mice. Beads coated with a higher concentration of L-selectin (L^{high}-microbeads) rolled equally well in HEV of core2$^{-/-}$ mice

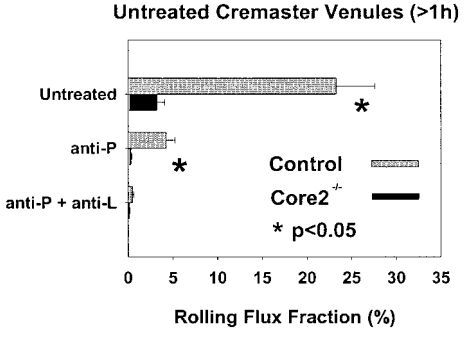

FIGURE 1. Leukocyte rolling flux fraction (mean ± SEM) in venules of the cremaster muscle of untreated Core2GlcNAcT-I-deficient mice (■) and control mice (▨) at >60 min after exteriorization. anti-P, mAb RB40.34; anti-L, mAb MEL-14. *, Significant differences ($p < 0.05$) in leukocyte rolling flux fraction between core2$^{-/-}$ and control groups.

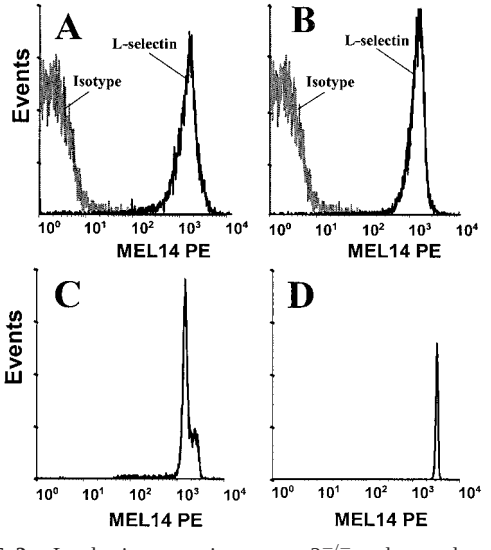

FIGURE 2. L-selectin expression on core2$^{-/-}$ and control neutrophils and on L-selectin-coupled beads. L-selectin expression was analyzed on neutrophils (gated by GR-1) by flow cytometry using PE-labeled L-selectin mAb MEL-14. A, Controls; B, core2$^{-/-}$ neutrophils (solid line) and isotype-controls (shaded line); C, L^{low} beads; D, L^{high} beads.

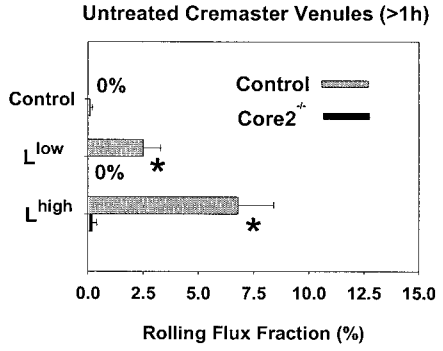

FIGURE 3. L-selectin-coated microbead rolling. Beads coated with L-selectin IgG chimera at 10 (L^{low}) and 100 (L^{high}) μg/ml roll in cremaster muscle venules of control mice (▨), but not of core2$^{-/-}$ mice (■). *, Significant differences ($p < 0.05$) in rolling flux fraction (mean ± SEM) between core2$^{-/-}$ and control groups.

(rolling flux fraction, 43%) and control mice (rolling flux fraction, 63%; Fig. 6). To demonstrate that bead rolling was specific for L-selectin, core2$^{-/-}$ mice and control mice were treated with the L-selectin-blocking mAb MEL-14 before injection of L^{high} beads. MEL-14 abolished rolling in both core2$^{-/-}$ mice and control mice,

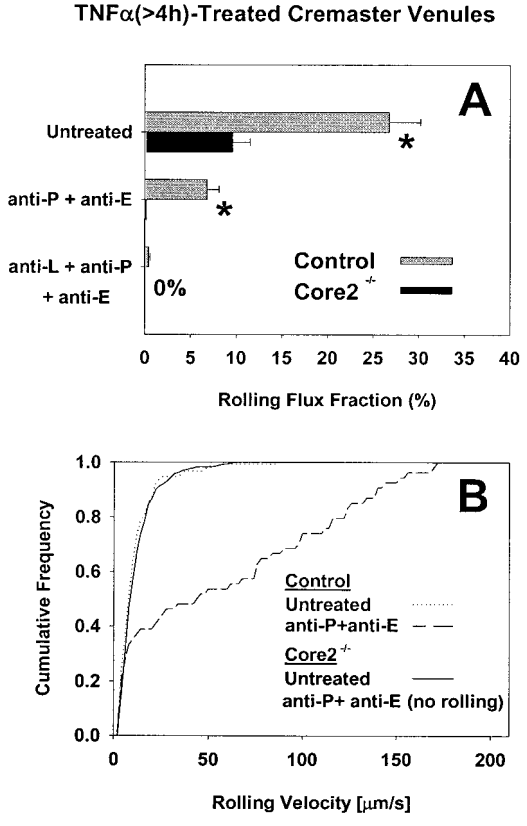

FIGURE 4. *A*, Leukocyte rolling flux fraction (mean ± SEM) in TNF-α-treated venules at >4 h in Core2GlcNAcT-I-deficient mice (■) and control mice (▨). anti-P, mAb RB40.34; anti-E, mAb 9A9; anti-L, mAb MEL-14. *, Significant differences ($p < 0.05$) in leukocyte rolling flux fraction between core2$^{-/-}$ and control mice. *B*, Leukocyte rolling velocity distribution in TNF-α-treated cremaster muscle venules. Cumulative histograms of leukocyte rolling velocities measured in cremaster muscle venules of core2$^{-/-}$ mice (——), control mice (·····), and control mice treated with P- and E-selectin-blocking mAbs RB40.34 (anti-P) and 9A9 (anti-E; – – –). Core2$^{-/-}$ mice treated with RB40.34 and 9A9 showed no rolling.

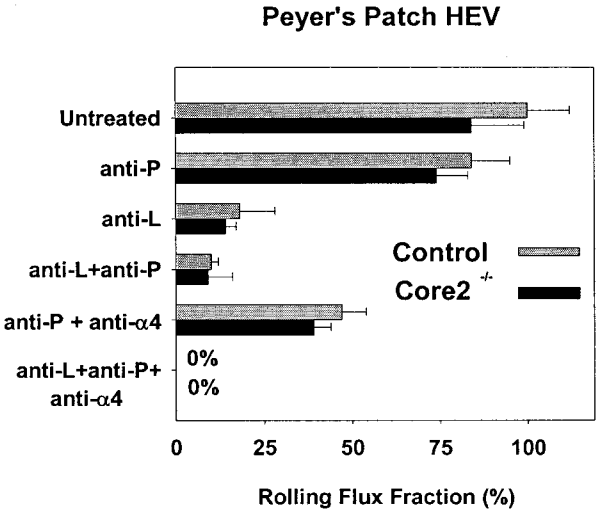

FIGURE 5. Leukocyte rolling flux fraction (mean ± SEM) in HEV of Peyer's patches of Core2GlcNAcT-I-deficient mice (■) and control mice (▨). anti-P, mAb RB40.34; anti-L, mAb MEL-14; anti-α_4, PS/2. *, No significant differences ($p < 0.05$) in leukocyte rolling flux fraction between core2$^{-/-}$ and control mice.

confirming that bead rolling is L-selectin mediated (Fig. 6). Taken together these findings suggest that L-selectin ligands in Peyer's patch HEV are slightly less efficient in core2$^{-/-}$ mice than in control mice. However, at the site density of L-selectin expressed on leukocytes in vivo, this does not lead to impaired rolling in Peyer's patch HEV.

Discussion

We show that L-selectin-dependent rolling of leukocytes and microbeads in venules of the untreated and TNF-α-treated cremaster muscle is absent in core2$^{-/-}$ mice, but not in control mice. This novel finding shows that Core2GlcNAcT-I is required for biosynthesis of functional L-selectin ligands in inflamed venules of the cremaster muscle. This shows that L-selectin ligands, like most P- and some E-selectin ligands (25, 38, 44) require modification by Core2GlcNAcT-I. Second, these findings unequivocally demonstrate that the relevant L-selectin ligands expressed on inflamed endothelial cells are *O*-linked glycans attached to mucin-like glycoproteins. This is significant, because the nature of L-selectin ligands on inflamed venules has remained elusive.

Previous studies have shown that L-selectin participates in leukocyte rolling in mesenteric and cremaster muscle venules (5, 7, 8,

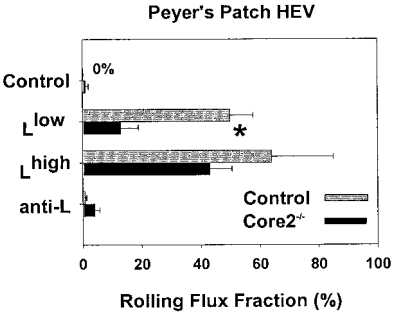

FIGURE 6. Rolling of control beads or L-selectin-coated beads (10 μg/ml for L^{low} and 100 μg/ml for L^{high}) on Peyer's patch HEV of Core2GlcNAcT-I-deficient mice (■) and control mice (▨). anti-L, mAb MEL-14. *, Significant differences ($p < 0.05$) in rolling flux fraction between core2$^{-/-}$ and control group.

15, 26). At least one of the candidate molecules, CD34, is not a major ligand for leukocyte rolling, because L-selectin-dependent rolling was normal in CD34$^{-/-}$ mice (45). A recent study reported that endothelial ligands for L-selectin bear the HECA-452 epitope (46), an indicator of post-translational modification by fucosyltransferase VII (47, 48). The present study reveals that these endothelial L-selectin ligands are completely Core2GlcNAcT-I dependent. This was confirmed with L-selectin-coated beads at low and high site densities. L-selectin ligands on inflamed endothelial cells are not functional when Core2GlcNAcT-I is absent.

The L-selectin ligands investigated here are physiologically important. First, an L-selectin-dependent pathway can mediate significant leukocyte accumulation in E/P$^{-/-}$ selectin double-knockout mice (8). Second, L-selectin-deficient mice have consistent reduction in leukocyte recruitment to inflammatory sites (15, 49). Some of this defect may be due to absence of secondary capture of leukocytes by other leukocytes, which is L-selectin dependent (50). Interestingly, the ligands responsible for leukocyte-leukocyte interactions through L-selectin are also Core2GlcNAcT-I dependent, because neutrophils from core2$^{-/-}$ mice do not roll on L-selectin (25). Our data demonstrate that L-selectin ligands on inflamed endothelium require modification by Core2GlcNAcT-I to support leukocyte or bead rolling and thus unequivocally show that these ligands are *O*-glycans.

In contrast to the findings in the cremaster muscle, leukocyte rolling in Peyer's patch HEV was not significantly different between Core2GlcNAcT-I-deficient mice and control mice. This is consistent with results showing normal secondary lymphoid organ size and structure in Core2GlcNAcT-I-deficient mice (25). Also, HEV in secondary lymphoid organs of core2$^{-/-}$ mice can be stained with an L-selectin IgM chimera (25). We found a partial reduction of rolling L-selectin IgG chimera-coupled beads (L^{low}) along the Peyer's patch HEV, which could not be observed after injection of L^{high} beads. Taking into account that L-selectin on leukocytes is concentrated in clusters on the tips of microvilli (51), these findings suggest that core2$^{-/-}$ mice exhibit a minor reduction in L-selectin ligand activity in Peyer's patch HEV, which does not lead to detectable impairment of lymphocyte homing. However, it cannot be excluded that homing may be reduced in lymphocyte subsets exhibiting low surface expression of L-selectin. Recent studies showed that B lymphocytes have a 30–50% lower surface expression of L-selectin than T lymphocytes (52). In addition, lymphocytes from hemizygous L-selectin$^{+/-}$ mice showed a 50% reduction in L-selectin expression, which resulted in a 40–50% decrease in short term lymphocyte migration into Peyer's patches (52). Earlier reports on leukocyte rolling in Peyer's patch HEV found that P-selectin contributes to rolling. However, this contribution appeared to be of minor significance (16). Our results demonstrate a modest, but not significant, reduction in leukocyte rolling on Peyer's patch HEV after injection of a P-selectin-blocking mAb. The observed reduction in rolling flux on Peyer's patch HEV in untreated core2$^{-/-}$ mice compared with control mice may relate to some impairment in P-selectin ligand function on lymphocytes and/or granulocytes (38). However, reduced rolling of L-selectin-coated beads in core2$^{-/-}$ mice clearly demonstrated a small impairment in L-selectin ligand function on HEV.

The cause of the differential reduction in L-selectin ligand function on inflamed endothelial cells, where L-selectin-mediated rolling is completely absent, compared with almost normal L-selectin ligand function on HEV of Peyer's patches is currently unknown. However, multiple Core2GlcNAcT-I exist, showing different tissue distribution and specificity. The first Core2GlcNAcT identified by transfection cloning is widely expressed, functions only in core2 synthesis (53, 54), and resembles the leukocyte Core2GlcNAcT activity identified by Williams and Schachter (55). The impact of absence of this enzyme on selectin ligand function was investigated here and in two previous reports (25, 38). Another Core2GlcNAcT was identified by expressed sequence tag cloning strategy and has a less restricted acceptor specificity (54, 56). It resembles the mucus Core2GlcNAcT activity and is mainly expressed in mucus-secreting organs (54, 56). It is thought that the leukocyte Core2GlcNAcT-I controls synthesis of core2-dependent selectin ligands in leukocytes and lymphoid tissues, but other, not yet identified, Core2GlcNAcT may exist. Recently, Schwientek et al. (57) cloned a novel Core2GlcNAcT, which shows a restricted expression pattern in human organs with high expression in thymus and weak expression in small intestine and peripheral blood leukocytes. In view of the fact that lymphoid tissue and lymphocyte homing are not significantly affected in Core2GlcNAcT-I mice as shown here and by Ellies et al. (25), it is possible that other forms of Core2GlcNAcT could account for selectin ligand function in lymphoid tissue. Another reason for the different L-selectin ligand function on inflamed endothelium and on HEV could lie in the existence of Core2GlcNAcT-I-independent selectin ligands as previously shown for P-selectin glycoprotein ligand-1-dependent rolling (38). Further research is needed to identify the molecular nature of the Core2GlcNAcT-I-independent L-selectin ligands.

In conclusion, the present study reveals a third mechanism by which the absence of Core2GlcNAcT-I impairs neutrophil recruitment to sites of inflammation, in addition to impaired P- and E-selectin ligand function (25, 38). L-selectin-dependent leukocyte or bead rolling at sites of inflammation is completely absent in core2$^{-/-}$ mice. In contrast, L-selectin-dependent leukocyte rolling in Peyer's patch HEV is not significantly impaired in core2$^{-/-}$ mice. These findings 1) unequivocally show that L-selectin ligands on inflamed endothelium are *O*-glycans; and 2) are fundamentally different from L-selectin ligands constitutively expressed in high endothelial venules. The knowledge that the relevant L-selectin ligands in inflammation are present on *O*-glycans should invigorate the search for the endothelial glycoproteins presenting these ligands.

Acknowledgments

We thank Drs. Ruth Eytner and Dietmar Vestweber (Universität Münster, Munster, Germany) for providing mAb RB40.34, and Dr. Barry Wolitzky for providing the E-selectin blocking Ab 9A9.

References

1. Butcher, E. C. 1991. Leukocyte-endothelial cell recognition: three (or more) steps to specificity and diversity. *Cell 67:1033.*
2. Springer, T. A. 1995. Traffic signals on endothelium for lymphocyte recirculation and leukocyte emigration. *Annu. Rev. Physiol. 57:827.*
3. Ley, K. 2001. Pathways and bottlenecks in the web of inflammatory adhesion molecules and chemoattractants. *Immunol. Res. In press.*
4. Kansas, G. S. 1996. Selectins and their ligands: current concepts and controversies. *Blood 88:3259.*
5. Ley, K., P. Gaehtgens, C. Fennie, M. S. Singer, L. A. Lasky, and S. D. Rosen. 1991. Lectin-like cell adhesion molecule 1 mediates leukocyte rolling in mesenteric venules in vivo. *Blood 77:2553.*
6. Von Andrian, U. H., J. D. Chambers, L. M. McEvoy, R. F. Bargatze, K.-E. Arfors, and E. C. Butcher. 1991. Two step model of leukocyte-endothelial cell interaction in inflammation: distinct roles for LECAM-1 and the leukocyte β_2 integrins in vivo. *Proc. Natl. Acad. Sci. USA 88:7538.*
7. Ley, K., T. F. Tedder, and G. S. Kansas. 1993. L-selectin can mediate leukocyte rolling in untreated mesenteric venules in vivo independent of E- or P-selectin. *Blood 82:1632.*
8. Jung, U., C. L. Ramos, D. C. Bullard, and K. Ley. 1998. Gene-targeted mice reveal importance of L-selectin-dependent rolling for neutrophil adhesion. *Am. J. Physiol. 274:H1785.*
9. Kunkel, E. J., and K. Ley. 1996. Distinct phenotype of E-selectin deficient mice: E-selectin is required for slow leukocyte rolling in vivo. *Circ. Res. 79:1196.*
10. Spertini, O., G. S. Kansas, J. M. Munro, J. D. Griffin, and T. F. Tedder. 1991. Regulation of leukocyte migration by activation of the leukocyte adhesion molecule-1 (LAM-1) selectin. *Nature 349:691.*
11. Tu, L., P. G. Murphy, X. Li, and T. F. Tedder. 1999. L-selectin ligands expressed by human leukocytes are HECA-452 antibody-defined carbohydrate epitopes

preferentially displayed by P-selectin glycoprotein ligand-1. *J. Immunol. 163: 5070.*
12. Zakrzewicz, A., M. Grafe, D. Terbeek, M. Bongrazio, W. Auch-Schwelk, B. Walzog, K. Graf, E. Fleck, K. Ley, and P. Gaehtgens. 1997. L-selectin-dependent leukocyte adhesion to microvascular but not to macrovascular endothelial cells of the human coronary system. *Blood 89:3228.*
13. Li, X., and T. F. Tedder. 1999. CHST1 and CHST2 sulfotransferases expressed by human vascular endothelial cells: cDNA cloning, expression, and chromosomal localization. *Genomics 55*.
14. Butcher, E. C., M. Williams, K. Youngman, L. Rott, and M. Briskin. 1999. Lymphocyte trafficking and regional immunity. *Adv. Immunol. 72:209.*
15. Arbones, M. L., D. C. Ord, K. Ley, H. Ratech, C. Maynard-Curry, G. Otten, D. J. Capon, and T. F. Tedder. 1994. Lymphocyte homing and leukocyte rolling and migration are impaired in L-selectin-deficient mice. *Immunity 1:247.*
16. Kunkel, E. J., C. L. Ramos, D. A. Steeber, W. Muller, N. Wagner, T. F. Tedder, and K. Ley. 1998. The roles of L-selectin, β_7 integrins, and P-selectin in leukocyte rolling and adhesion in high endothelial venules of Peyer's patches. *J. Immunol. 161:2449.*
17. Varki, A. 1994. Selectin ligands. *Proc. Natl. Acad. Sci. USA 91:7390.*
18. Cummings, R. D., and J. B. Lowe. 1999. Selectins. In *Essentials of Glycobiology*. A. Varki, R. D. Cummings, J. D. Esko, H. H. Freeze, G. Hart, and J. D. Marth, eds. Cold Spring Harbor Laboratory Press, Cold Spring Harbor, p. 391.
19. Imai, Y., L. A. Lasky, and S. D. Rosen. 1993. Sulphation requirement for GlyCAM-1, an endothelial ligand for L-selectin. *Nature 361:555.*
20. Hemmerich, S., and S. D. Rosen. 2000. Carbohydrate sulfotransferases in lymphocyte homing. *Glycobiology 10:849.*
21. Hemmerich, S., E. C. Butcher, and S. D. Rosen. 1994. Sulfation-dependent recognition of high endothelial venules (HEV)-ligands by L-selectin and MECA 79, an adhesion-blocking monoclonal antibody. *J. Exp. Med. 180:2219.*
22. Vestweber, D., and J. E. Blanks. 1999. Mechanisms that regulate the function of the selectins and their ligands. *Physiol. Rev. 79:181.*
23. Maly, P., A. D. Thall, B. Petryniak, C. E. Rogers, P. L. Smith, R. M. Marks, R. J. Kelly, K. M. Gersten, G. Cheng, T. L. Saunders, et al. 1996. The α(1,3)fucosyltransferase Fuc-TVII controls leukocyte trafficking through an essential role in L-, E-, and P-selectin ligand biosynthesis. *Cell 86:643.*
24. Weninger, W., L. H. Ulfman, G. Cheng, N. Souchkova, E. J. Quackenbush, J. B. Lowe, and U. H. von Andrian. 2000. Specialized contributions by α(1, 3)-fucosyltransferase-IV and FucT-VII during leukocyte rolling in dermal microvessels. *Immunity 12:665.*
25. Ellies, L. G., S. Tsuboi, B. Petryniak, J. B. Lowe, M. Fukuda, and J. D. Marth. 1998. Core2 oligosaccharide biosynthesis distinguishes between selectin ligands essential for leukocyte homing and inflammation. *Immunity 9:881.*
26. Ley, K., D. C. Bullard, M. L. Arbones, R. Bosse, D. Vestweber, T. F. Tedder, and A. L. Beaudet. 1995. Sequential contribution of L- and P-selectin to leukocyte rolling in vivo. *J. Exp. Med. 181:669.*
27. Bosse, R., and D. Vestweber. 1994. Only simultaneous blocking of the L- and P-selectin completely inhibits neutrophil migration into mouse peritoneum. *Eur. J. Immunol. 24:3019.*
28. Berlin, C., R. F. Bargatze, J. J. Campbell, U. H. von Andrian, M. C. Szabo, S. R. Hasslen, R. D. Nelson, E. L. Berg, S. L. Erlandsen, and E. C. Butcher. 1995. α_4 integrins mediate lymphocyte attachment and rolling under physiologic flow. *Cell 80:413.*
29. Hamann, A., D. P. Andrew, D. Jablonski-Westrich, B. Holzmann, and E. C. Butcher. 1994. Role of α_4 integrins in lymphocyte homing to mucosal tissues in vivo. *J. Immunol. 152:3282.*
30. Watson, S. R., Y. Imai, C. Fennie, J. S. Geoffroy, S. D. Rosen, and L. A. Lasky. 1990. A homing receptor-IgG chimera as a probe for adhesive ligands of lymph node high endothelial venules. *J. Cell Biol. 110:2221.*
31. Bargatze, R. F., M. A. Jutila, and E. C. Butcher. 1995. Distinct roles of L-selectin and integrins $\alpha_4\beta_7$ and LFA-1 in lymphocyte homing to Peyer's patch-HEV in situ: the multistep model confirmed and refined. *Immunity 3:99.*
32. Wagner, N., J. Löhler, E. J. Kunkel, K. Ley, E. Leung, G. Krissansen, K. Rajewsky, and W. Müller. 1996. Critical role for β_7 integrins in formation of the gut-associated lymphoid tissue. *Nature 382:366.*
33. Pries, A. R. 1988. A versatile video image analysis system for microcirculatory research. *Int. J. Microcirc. Clin. Exp. 7:327.*
34. Lipowsky, H. H., and B. W. Zweifach. 1978. Application of the "two-slit" photometric technique to the measurement of microvascular volumetric flow rates. *Microvasc. Res. 15:93.*
35. Reneman, R. S., B. Woldhuis, M. G. A. oude Egbrink, D. W. Slaaf, and G. J. Tangelder. 1992. Concentration and velocity profiles of blood cells in the microcirculation. In *Advances in Cardiovascular Engineering*. N. H. C. Hwang, V. T. Turitto, and M. R. T. Yen, eds. Plenum Press, New York, p. 25.
36. Ley, K., A. R. Pries, and P. Gaehtgens. 1988. Preferential distribution of leukocytes in rat mesentery microvessel networks. *Pfluegers Arch. 412:93.*
37. Ley, K., J. U. Meyer, M. Intaglietta, and K.-E. Arfors. 1989. Shunting of leukocytes in rabbit tenuissimus muscle. *Am. J. Physiol. 256:H85.*
38. Sperandio, M., Thatte, A., D. S. Foy, L. G. Ellies, J. D. Marth, and K. Ley. 2001. Severe impairment of leukocyte rolling in venules of leukocyte core2 β1,6-*N*-acetylglucosaminyltransferase deficient mice. *Blood 97:3814.*
39. Mayadas, T. N., R. C. Johnson, H. Rayburn, R. O. Hynes, and D. D. Wagner. 1993. Leukocyte rolling and extravasation are severely compromised in P selectin-deficient mice. *Cell 74:541.*
40. Jung, U., D. C. Bullard, T. F. Tedder, and K. Ley. 1996. Velocity difference between L-selectin and P-selectin dependent neutrophil rolling in venules of the mouse cremaster muscle in vivo. *Am. J. Physiol. 271:H2740.*
41. Scharffetter-Kochanek, K., H. F. Lu, K. Norman, N. Vannood, F. Munoz, S. Grabbe, M. McArthur, I. Lorenzo, S. Kaplan, K. Ley, et al. 1998. Spontaneous skin ulceration and defective T cell function in CD18 null mice. *J. Exp. Med. 188:119.*
42. Bullard, D. C., E. J. Kunkel, H. Kubo, M. J. Hicks, I. Lorenzo, N. A. Doyle, C. M. Doerschuk, K. Ley, and A. L. Beaudet. 1996. Infectious susceptibility and severe deficiency of leukocyte rolling and recruitment in E-selectin and P-selectin double mutant mice. *J. Exp. Med. 183:2329.*
43. Jung, U., and K. Ley. 1997. Regulation of E-selectin, P-selectin and ICAM-1 expression in mouse cremaster muscle vasculature. *Microcirculation 4:311.*
44. Snapp, K. R., Heitzig, C. E., L. G. Ellies, J. D. Marth, and G. S. Kansas. 2001. Differential requirements for the *O*-linked branching enzyme core2 β1,6-*N*-glucosaminyltransferase (C2GlcNAcT-1(L)) in biosynthesis of ligands for E-selectin and P-selectin. *Blood 97:000.*
45. Suzuki, A., D. P. Andrew, J.-A. Gonzalo, M. Fukumoto, J. Spellberg, M. Hashiyama, T. Suda, H. Takimoto, N. Gerwin, J. Webb, et al. 1996. CD34 deficient mice have reduced eosinophil accumulation after allergen exposure and reveal a novel crossreactive 90 kD protein. *Blood 87:3550.*
46. Tu, L., M. D. Delahunty, H. Ding, F. W. Luscinskas, and T. F. Tedder. 1999. The cutaneous lymphocyte antigen is an essential component of the L-selectin ligand induced on human vascular endothelial cells. *J. Exp. Med. 189:241.*
47. Wagers, A. J., L. M. Stoolman, R. Kannagi, R. Craig, and G. S. Kansas. 1997. Expression of leukocyte fucosyltransferases regulates binding to E-selectin: relationship to previously implicated carbohydrate epitopes. *J. Immunol. 159:1917.*
48. Knibbs, R. N., R. A. Craig, S. Natsuka, A. Chang, M. Cameron, J. B. Lowe, and L. M. Stoolman. 1996. The fucosyltransferase FucT-VII regulates E-selectin ligand synthesis in human T cells. *J. Cell Biol. 133:911.*
49. Tedder, T. F., D. A. Steeber, and P. Pizcueta. 1995. L-selectin deficient mice have impaired leukocyte recruitment into inflammatory sites. *J. Exp. Med. 181:2259.*
50. Bargatze, R. F., S. Kurk, E. C. Butcher, and M. A. Jutila. 1994. Neutrophils roll on adherent neutrophils bound to cytokine-induced endothelial cells via L-selectin on the rolling cells. *J. Exp. Med. 180:1785.*
51. Von Andrian, U. H., S. R. Hasslen, R. D. Nelson, S. L. Erlandsen, and E. C. Butcher. 1995. A central role for microvillous receptor presentation in leukocyte adhesion under flow. *Cell 82:989.*
52. Tang, M. L., D. A. Steeber, X. Q. Zhang, and T. F. Tedder. 1998. Intrinsic differences in L-selectin expression levels affect T and B lymphocyte subset-specific recirculation pathways. *J. Immunol. 160:5113.*
53. Bierhuizen, M. F., and M. Fukuda. 1992. Expression cloning of a cDNA encoding UDP-GlcNAc:Gal b1–3-GalNAc-R (GlcNAc to GalNAc) β1–6GlcNAc transferase by gene transfer into CHO cells expressing polyoma large tumor antigen. *Proc. Natl. Acad. Sci. USA 89:9326.*
54. Yeh, J. C., Ong, E., and M. Fukuda. 1999. Molecular cloning and expression of a novel β-1,6-*N*-acetylglucosaminyltransferase that forms core2, core 4, and I branches. *J. Biol. Chem. 274:3215.*
55. Williams, D., and H. Schachter. 1980. Mucin synthesis. I. Detection in canine submaxillary glands of an *N*-acetylglucosaminyltransferase which acts on mucin substrates. *J. Biol. Chem. 255:11247.*
56. Schwientek, T., M. Nomoto, S. B. Levery, G. Merkx, A. G. van Kessel, E. P. Bennett, M. A. Hollingsworth, and H. Clausen. 1999. Control of *O*-glycan branch formation: molecular cloning of human cDNA encoding a novel β1,6-*N*-acetylglucosaminyltransferase forming core2 and core4. *J. Biol. Chem. 274:4504.*
57. Schwientek, T., J. C. Yeh, S. B. Levery, B. Keck, G. Merkx, A. G. van Kessel, M. Fukuda, and H. Clausen. 2000. Control of *O*-glycan branch formation: molecular cloning and characterization of a novel thymus-associated core2 β1,6-*N*-acetylglucosaminyltransferase. *J. Biol. Chem. 275:11106.*